LA-UR-01-2484
Approved for public release;
distribution is unlimited.

Title: **Hybrid and Hall-MHD Simulations of Collisionless Reconnection: Effects of Plasma Pressure Tensor**

Author(s): **Lin Yin, Dan Winske, S. Peter Gary, and Joachim Birn**

Submitted to:

http://lib-www.lanl.gov/la-pubs/00796071.pdf

Proceedings of ISSS-6 (2001): 1–4 © Copernicus Gesellschaft 2001

ISSS–6

Hybrid and Hall-MHD Simulations of Collisionless Reconnection: Effects of Plasma Pressure Tensor

Lin Yin[1], **Dan Winske**[1], **S. Peter Gary**[2], **and Joachim Birn**[2]

[1]Applied Physics Division, Los Alamos National Laboratory, Los Alamos, New Mexico, USA
[2]Space and Atmospheric Sciences, Los Alamos National Laboratory, Los Alamos, New Mexico, USA

Abstract. In this study we performed two-dimensional hybrid (particle ions, massless fluid electrons) and Hall-MHD simulations of collisionless reconnection in a thin current sheet. Both calculations include the full electron pressure tensor (instead of a localized resistivity) in the generalized Ohm's law to initiate reconnection, and in both an initial perturbation to the Harris equilibrium is applied. First, electron dynamics from the two calculations are compared, and we find overall agreement between the two calculations in both the reconnection rate and the global configuration. To address the issue of how kinetic treatment for the ions affects the reconnection dynamics, we compared the fluid-ion dynamics from the Hall-MHD calculation to the particle-ion dynamics obtained from the hybrid simulation. The comparison demonstrates that off-diagonal elements of the ion pressure tensor are important in correctly modeling the ion out-of-plane momentum transport from the X point. It is shown that these effects can be modeled efficiently using a particle Hall-MHD simulation method in which particle ions are used in a predictor/corrector to implement the ion gyroradius corrections. We also investigate the micro- macroscale coupling in the magnetotail dynamics by using a new integrated approach in which particle Hall-MHD calculations are embedded inside a MHD simulation. Initial results of the embedded simulation concerning current sheet thinning and reconnection dynamics are discussed.

1 Introduction

Fast magnetic reconnection, or the rapid change of magnetic topology and release of magnetic energy, is a fundamental and ubiquitous process in plasma physics. It arises in many plasma phenomena, for example, solar flares, the dynamics of the Earth's magnetotail during a geomagnetic substorm, and disruptions in laboratory fusion experiments. During fast reconnection, the magnetic field self-annihilates in regions where the field reverses direction, and the stored magnetic energy is released explosively and is converted to particle acceleration and heating. Although initiated in a localized region near a topological X point, reconnection dramatically changes the field configuration and the particle orbits on a large-scale and is an important plasma transport process.

In order for reconnection to occur, a dissipative electric field near the X point is required. An expression for the electric field, the generalized Ohm's law, is obtained from the electron momentum equation:

$$\boldsymbol{E} = -\boldsymbol{v}_{\rm i} \times \boldsymbol{B} + \frac{1}{en_e}(\boldsymbol{J} \times \boldsymbol{B} - \boldsymbol{\nabla} \cdot \mathbf{P}_e) - \frac{m_e}{e}\frac{d\boldsymbol{v}_{\rm e}}{dt} + \eta \boldsymbol{J} \,.$$

The first term is the ideal MHD approximation, in which ions and electrons are frozen into and convect together with the magnetic flux. However, at the ion inertial length scale near the X point, the Hall term (the second term) becomes important. Combining the first and second terms yields $-\boldsymbol{v}_{\rm e} \times \boldsymbol{B}$. This means that electrons are magnetized and are convecting with the magnetic field, while ions are unmagnetized. Thus, at the ion inertial length scale near the X point, ion and electron motions decouple. Since the magnetic field vanishes at the X point, these terms containing the magnetic field do not contribute to the reconnection electric field. The dissipative electric field near the X point required for reconnection is provided by the divergence of the electron pressure tensor at the ion inertial length scale (Hesse and Winske, 1994; Kuznetsova et al., 2000), or by the electron inertia at the electron inertial scale (Drake et al., 1997; Biskamp et al., 1997; Shay et al., 2001). It has been concluded from hybrid and full particle simulations that the electron pressure tensor contribution to the reconnection electric field dominates the electron inertia contribution (Hesse and Winske, 1998; Kuznetsova et al., 2000; Pritchett, 2001). In a collisionless plasma, resistivity from particle-particle collisions is absent, and anomalous resistivity arising from wave-particle collisions is inadequate, thus the last resistive term can be neglected. Nevertheless, the resistive term has been used as a simplified model to replace the electron pressure tensor term

Correspondence to: lyin@lanl.gov

or the electron inertia term.

Various plasma simulation methods, e.g., full-particle (kinetic ions and electrons), hybrid (kinetic ions, fluid electrons), two-fluid Hall-MHD, and resistive MHD have been employed in studying reconnection dynamics near the X point, for example, in the recent Geospace Environment Modeling (GEM) reconnection challenge studies (Birn et al., 2001; Hesse et al., 2001; Kuznetsova et al., 2001; Ma and Bhattacharjee, 2001; Pritchett, 2001; Shay et al., 2001). An important result of the GEM study and subsequent research is that the Hall current is essential to the reconnection dynamics and that the reconnection rate is independent of the mechanism, that is, the divergence of the electron pressure tensor, electron inertia, or resistivity, that provides the dissipative electric field near the X point.

In the present work, collisionless reconnection in a thin current sheet is further studied using two-dimensional hybrid and Hall-MHD simulations. Both calculations include the full electron pressure tensor in the generalized Ohm's law to initiate reconnection. We neglect resistivity and electron inertia in this work, so the last two terms in Ohm's law vanish. The time-varying full electron pressure tensor $\mathbf{P}_e$ is computed based on the following equation (Hesse and Winske, 1994):

$$\frac{\partial \mathbf{P}_e}{\partial t} = -\boldsymbol{v}_{\rm e}\cdot\boldsymbol{\nabla}\mathbf{P}_e - \mathbf{P}_e\boldsymbol{\nabla}\cdot\boldsymbol{v}_{\rm e} - \mathbf{P}_e\cdot\boldsymbol{\nabla}\boldsymbol{v}_{\rm e} - (\mathbf{P}_e\cdot\boldsymbol{\nabla}\boldsymbol{v}_{\rm e})^T - \frac{\Omega_e}{\tau}(\mathbf{P}_e - p\mathbf{1})\,.$$

In this expression, Ω_e is the electron gyrofrequency, the superscript T is the transpose of the matrix, and $p = \frac{1}{3}\mathrm{Tr}(\mathbf{P}_e)$. The last term on the right-hand side of this equation represents the reduction of the nongyrotropic (off-diagonal) elements of the electron pressure tensor and the isotropization of the three diagonal elements, and τ is a parameter corresponding to a gyrotropization/isotropization time of the order of electron cyclotron time.

The Hall-MHD code was developed with numerical methods similar to those used in conventional hybrid codes (Winske and Quest, 1988; Hesse and Winske, 1994) so that direct comparison of the results of the two codes could more easily be carried out. Spatial grid quantities in both codes are defined on the same set of staggered finite-difference meshes, where the magnetic field components are defined at the centers of the squares and all other quantities are defined at the squares' vertices. The time differencing follows a conventional staggered leapfrog method. In the hybrid simulation, $\boldsymbol{E}$ and $\boldsymbol{B}$ are advanced in time with a predictor-corrector scheme (Winske and Quest, 1986). In the Hall-MHD code the magnetic field $\boldsymbol{B}$ is advanced in time using a fourth-order Runge-Kutta scheme with subcycling (Winske and Quest, 1988). In each time step used to advance the fluid moments (velocity, density, and pressure), five to ten substeps are used, typically, to update the fields. In our Hall-MHD code a smoothing routine is used instead of the conventional second-order viscosity (i.e., $\sim \nu\nabla^2\boldsymbol{v}$); a sixth order hyperviscous dissipation, $\sim \nu(\nabla^6{}_x + \nabla^6{}_y)\boldsymbol{B}$, is employed in the magnetic field equation to damp out fluctuations on very short spatial scales,

The simulations are performed in the (x, y) plane in which $\hat{x}$ is the direction normal to the sheet and $\hat{y}$ is along the sheet. Both calculations employ an initial perturbation to the Harris equilibrium $B_y = B_o \tanh\{[x - l_x/2]/\alpha\}$, where l_x is the width of the simulation domain and α is the half-thickness of the current sheet. The perturbed normal magnetic field $B_x \sim \sin\{2\pi[y - l_y/2]/l_y\}\exp\{-[x - l_x/2]^2/\alpha^2\}$, where l_y is the length of the simulation domain, ensures the system evolves into a nonlinear stage quickly. The boundary conditions are periodic on the y-boundaries; on the x-boundaries the velocity and field components transverse to the local magnetic field vanish. The hybrid calculation includes uniform background ions whose temperature is the same as the sheet ions. The lobe plasma beta is 0.2, $T_i/T_e = 5$ initially. We use $\alpha = 0.4$ for a 10×10 $(c/\omega_{\rm pi})^2$ domain with 128×128 grids, and $\alpha = 0.8$ for a 20×20 $(c/\omega_{\rm pi})^2$ domain with 256×256 grids.

2 Electron Dynamics

As in the GEM reconnection challenge studies, we find overall agreement between the two calculations in the reconnection rate, the global configuration of the currents and the fields, and the properties of the electron pressure (Yin et al., 2001a). Here we use our Hall-MHD simulation results to demonstrate the scale separations from Ohm's law. In Figure 1, the in-plane magnetic field lines are overlaid on the color contours of the electric field E_z (E_z have positive values in the red regions and negative values in the blue regions). The scale size of the localized region at the X point where the off-diagonal terms of the electron pressure tensor contribution $-(\partial P^{\,e}_{\rm xz}/\partial x + \partial P^{\,e}_{\rm yz}/\partial y)$ peaks in the $\hat{z}$ direction is indicated by the top panel. As a comparison, the spatial structure of the E_z from the Hall term $(1/en)(J_x \times B_y - J_y \times B_x)$ is depicted in the middle panel. It shows that while the electron pressure tensor effect is important at the X point, in the surrounding regions the magnetic field strength becomes finite, and the Hall term provides the dominant contribution to E_z. Since the z component of the Hall term is related to the disparities in the ion and electron x and y velocities, the red region surrounding the X point in the middle panel indicates the region where the electron flow leads the ion flow and the current is carried by the electrons; in contrast, in the blue regions at the center of the sheet extending toward the O points the ion outflow leads that of the electrons and the ions become the current carriers. Other outer regions where the ion dynamics contribute are shown in the bottom panel, in which the color-coded magnitude of $-(\boldsymbol{v}_{\rm i} \times \boldsymbol{B})$ is plotted.

Results of this study show that in addition to providing the reconnection electric field at the X point the divergence of the electron pressure tensor leads to in-plane electric fields that exert drag forces on the ions as they enter and exit the near-X-point region. The in-plane electric fields are enhanced in regions of small transverse scale along the edge of the sheet,

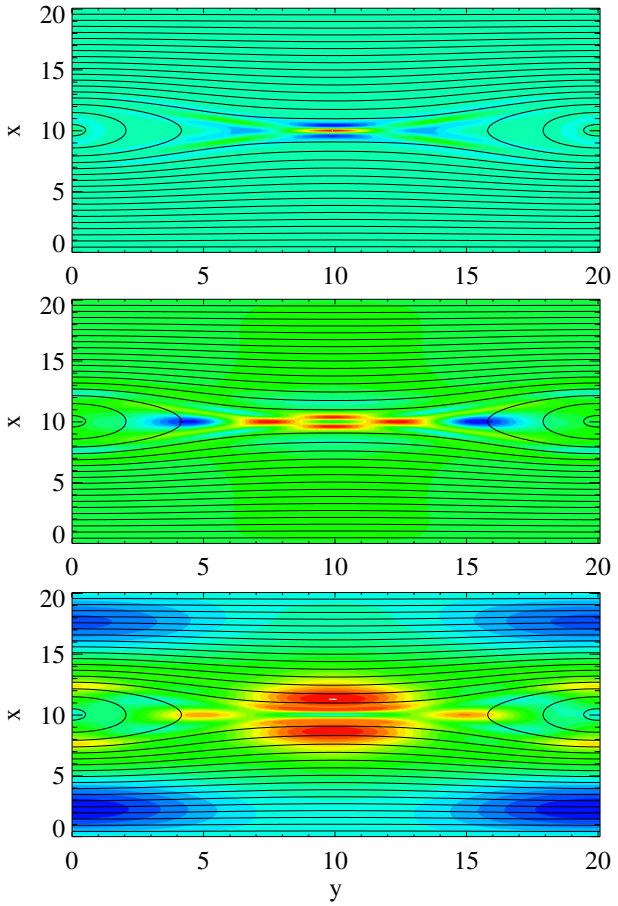

Fig. 1. Individual contributions to the E_z electric field from a Hall-MHD run ($t\,\Omega_{\rm ci} = 30$): (top panel) $E_z \sim -(1/en)(\partial P^{\,e}_{\rm xz}/\partial x + \partial P^{\,e}_{\rm yz}/\partial y)$, (middle) $E_z \sim (1/en)(J_x \times B_y - J_y \times B_x)$, and (bottom) $E_z \sim -(\mathrm{v_i} \times \mathrm{B})$. The minimum and maximum values for the top, middle, and bottom panels are (-0.022, 0.050), (-0.024, 0.030), and (-0.015, 0.041), respectively.

and the resulting narrow electron current layers are demonstrated clearly.

3 Ion Dynamics and Particle Hall-MHD Simulation

Comparison of the ion dynamics from the two types of simulations reveals that while the ion density and ion in-plane velocities v_x and v_y from the two calculations are in general agreement, the spatial configuration of the out-of-plane ion velocity v_z shows a significant difference. The global structure of v_z from the hybrid simulation indicates a reduction of the ion z-momentum at the X point as reconnection proceeds. In contrast, the spatial configuration of v_z from the Hall-MHD run remains peaked at the X point at the end of the run. This difference is clearly seen by comparing the top panel (v_z from the hybrid run) to the middle panel (v_z from the Hall-MHD run) in Figure 2. The lack of z-momentum transport in the Hall run is due to the absence of the ion gyro-orbits. In the reconnection field E_z the ions at the X point are accelerated and gain z-momentum. As the ions move out of the X point, they gyrate in the reconnection B_x field with an average gyro-radius of several $c/\omega_{\rm pi}$ and with their gyro-motion slow compared to their bounce motion between the two lobes. These ions undergo Speiser-like motion and contribute to a slanted component in the (v_y, v_z) ion distribution. These non-gyrotropic ion distributions are found in our hybrid simulation in the central region of the sheet away from the X point but within a few ion inertial lengths from the X point. This results in a finite off-diagonal term $P^{\,i}_{\rm yz}$ of the ion pressure tensor in these regions.

In the Hall-MHD code ion dynamics are described by the ion momentum equation with a scalar ion pressure P_i. We modify the ion momentum equation to include the ion pressure tensor $\mathbf{P}_i$ term to model ion gyro-radius effects:

$$nm_i \frac{\partial \boldsymbol{v}_{\rm i}}{\partial t} = -nm_i(\boldsymbol{v}_{\rm i} \cdot \boldsymbol{\nabla})\,\boldsymbol{v}_{\rm i} - \boldsymbol{\nabla}\cdot\mathbf{P}_i - \boldsymbol{\nabla}\cdot\mathbf{P}_e + \frac{\boldsymbol{J}\times\boldsymbol{B}}{c}\,.$$

The second term on the right has a component in the z direction which is $-(\partial P^{\,i}_{\rm yz}/\partial y + \partial P^{\,i}_{\rm xz}/\partial x)$. It affects the ion out-of-plane momentum balance.

Ion gyro-radius corrections are introduced in our Hall-MHD code using particle ions in a predictor/corrector manner to implement the ion gyro-radius corrections and to model correctly the z momentum transport (Yin et al., 2001b). In the Hall-MHD code, ions that are in initial pressure equilibrium with the fields are loaded and advanced in the Hall-MHD fields at every time step. For each ion species (i.e., the sheet ions and the background ions), its pressure tensor is defined in the center of mass frame

$$\mathbf{P}^o_s = m_s \int [\boldsymbol{v} - \langle \boldsymbol{v}_{\rm O}\rangle]\,[\boldsymbol{v} - \langle \boldsymbol{v}_{\rm O}\rangle] f_s(\boldsymbol{v}) d^3\boldsymbol{v}\,,$$

where $\langle \boldsymbol{v}_{\rm O}\rangle = \sum m_s n_s \langle \boldsymbol{v}_{\rm S}\rangle / \sum m_s n_s$ is the center of mass velocity. The $P^{\,i}_{\rm yz}$ and $P^{\,i}_{\rm xz}$ moments are weighted from the two species contributions and are accumulated onto the grid at every time step. These terms are used to modified the the ion momentum equation to include the ion gyro-radius effects. The corrected z momentum is then used to compute the fields at the next time step. The spatial structures of the $P^{\,i}_{\rm yz}$ and $P^{\,i}_{\rm xz}$ obtained from the ion particles pushed in the Hall-MHD fields are in agreement with those from our hybrid simulations, and they are consistent with full particle results (Cai et al., 1994).

The bottom panel in Figure 2 shows v_z from the particle Hall-MHD simulation. The ion gyro-radius correction allows the z momentum transport from the X point, and the v_z panel from the particle Hall-MHD run is consistent with that of the hybrid run shown in the top panel. Since ions control the overall reconnection dynamics, this correction affects the reconnection rate. The particle Hall-MHD run is shown to improve the average reconnection rate compared with the hybrid result. We found that the improvement the particle Hall-MHD simulation made is primarily due to the $P^{\,i}_{\rm yz}$ correction.

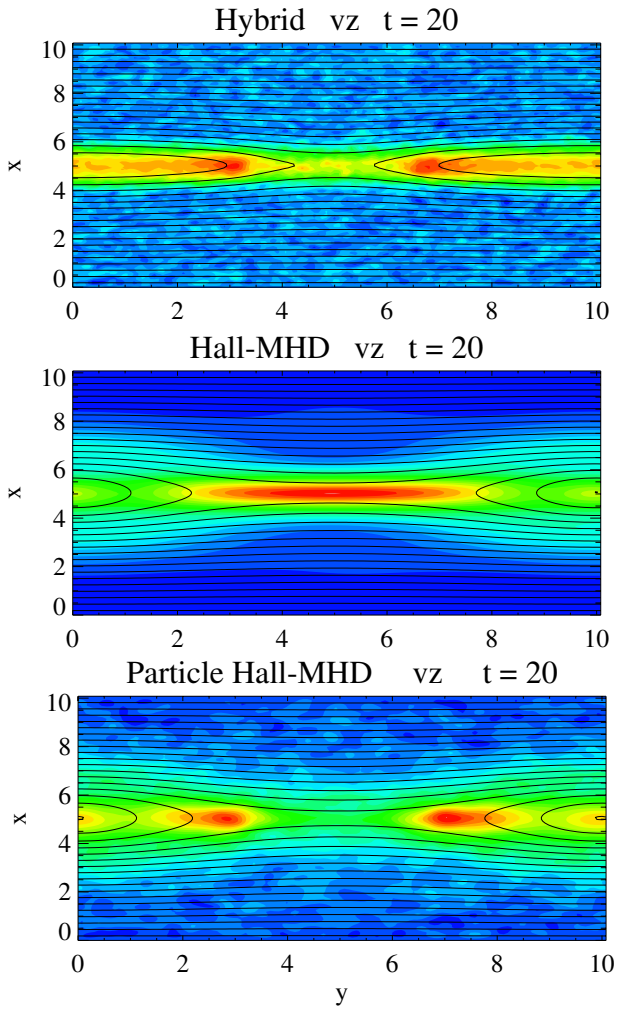

Fig. 2. The global configuration of the out-of-plane ion velocity from the hybrid simulation (top panel), the Hall-MHD simulation with scalar ion pressure (middle), and the particle Hall-MHD simulation (bottom).

4 Embedding of Particle Hall-MHD Calculations Within a MHD Simulation

We have shown that the essential small-scale physics and ion kinetic effects of reconnection can be modeled through this particle Hall-MHD simulation. This simulation method includes the full electron pressure tensor in the generalized Ohm's law to initiate reconnection and uses particle ions to implement the ion gyro-radius corrections and to model correctly the z momentum transport. The particle Hall-MHD simulation method presented in this work can be implemented in fluid models of magnetotail reconnection to improve the fidelity of the model in describing small-scale and ion kinetic processes near the X point. We investigate the micro- macroscale coupling in the magnetotail dynamics by using a new integrated approach in which particle Hall-MHD calculations are embedded inside a MHD simulation in the region near the X point. The MHD solution provides appropriate boundary conditions for the electric and magnetic fields as well as particle fluxes on the boundaries. The Hall-MHD code then runs on the inner region with an appropriately reduced time step and then provide revised boundary data for the MHD code at the next MHD time step. Initial results of the embedded simulation concerning current sheet thinning and reconnection dynamics are discussed.

Acknowledgements. This research was performed under the auspices of the U.S. Department of Energy and was supported in part by the National Aeronautics and Space Administration, the Sun-Earth Connection Theory Program. L. Y. gratefully acknowledges support provided by a Los Alamos National Laboratory, Director's Postdoctoral Fellowship.

References

Birn, J., et al., Geospace Environment Modeling (GEM) magnetic reconnection challenge, J. Geophys. Res., 106, 3715, 2001.

Biskamp, D., Schwarz, E., and Drake, J. F., Two-fluid theory of collisionless magnetic reconnection, Phys. Plasmas, 4, 1002, 1997.

Cai, H. J., Ding, D. Q., and Lee, L. C., Momentum transport near a magnetic X line in collisionless reconnection, J. Geophys. Res., 99, 35, 1994.

Drake, J. F., Biskamp, D., and Zeiler, A., Breakup of the electron current layer during 3-D collisionless magnetic reconnection, Geophys. Res. Lett., 24, 2921, 1997.

Hesse, M. and Winske, D., Hybrid simulations of collisionless reconnection in current sheets, J. Geophys. Res., 99, 11177, 1994.

Hesse, M. and Winske, D., Electron dissipation in collisionless magnetic reconnection, J. Geophys. Res., 103, 26,479, 1998.

Hesse, M., Birn, J., and Kuznetsova, M., Collisionless magnetic reconnection: Electron processes and transport modeling, J. Geophys. Res., 106, 3721, 2001.

Kuznetsova, M. M., Hesse, M., and Winske, D., Toward a transport model of collisionless magnetic reconnection, J. Geophys. Res., 105, 7601, 2000.

Kuznetsova, M. M., Hesse, M., and Winske, D., Collisionless reconnection supported by nongyrotropic pressure effects in hybrid and particle simulations, J. Geophys. Res., 106, 3799, 2001.

Ma, Z. W. and Bhattacharjee, A., Hall magnetohydrodynamic reconnection: The Geospace Environment Modeling challenge, J. Geophys. Res., 106, 3773, 2001.

Pritchett, P. L., Geospace Environment Modeling magnetic reconnection challenge: Simulations with a full particle electromagnetic code, J. Geophys. Res., 106, 3783, 2001.

Shay, M. A., Drake, J. F., Rogers, B. N., and Denton, R. E., Alfvénic collisionless magnetic reconnection and the Hall term, J. Geophys. Res., 106, 3759, 2001.

Winske, D. and Quest, K. B., Electromagnetic ion beam instabilities: Comparison of one- and two-dimensional simulations, J. Geophys. Res., 91, 8789, 1986.

Winske, D. and Quest, K. B., Magnetic field and density fluctuations at perpendicular supercritical collisionless shocks, J. Geophys. Res., 93, 9681, 1988.

Yin, L., Winske, D., Gary, S. P., and Birn, J., Hybrid and Hall-MHD simulations of collisionless reconnection: Dynamics of the electron pressure tensor, J. Geophys. Res., in press, 2001a.

Yin, L., Winske, D., Gary, S. P., and Birn, J., Particle Hall-MHD simulation of collisionless reconnection: Ion gyro-radius correction, Geophys. Res. Lett., in press, 2001b.